（昭和 56 年 11 月　日本造船学会秋季講演会において講演）

Free Surface Shock Waves and Methods for Hull Form Improvement

(First Report)

by Masao Nito*, *Member*　Hisashi Kajitani**, *Member*
Hideaki Miyata**, *Member*　Yoshihiro Tsuchiya**

Summary

A new method of designing hull forms of minimum wave resistance is developed in which two major components of wave resistance, i.e., one due to free surface shock waves and the other due to linear waves are taken into account. A procedure of extracting wave profiles due to free surface shock waves is proposed, which is utilized as a quantitative measure of the magnitude of free surface shock waves. The relation between hull form and resistance coefficient due to free surface shock waves is empirically derived and it is incorporated into the wave-analytical procedure of obtaining hull forms of minimum wave pattern resistance, so that the sum of wave pattern resistance (linear wave resistance) and resistance due to free surface shock waves (nonlinear wave resistance) is minimized. The effectiveness of the new method is demonstrated by experiments.

1. Introduction

The characteristics of Free Surface Shock Wave (abbreviated as FSSW) found and investigated at the Experimental Tank of the University of Tokyo are entirely different from those of linear dispersive waves (Kelvin waves). The nonlinear characteristics of FSSW described in the references provide strong barriers against crucial and analytical evaluation of the resistance due to FSSWs, and it may only be achieved by a somewhat tedious numerical procedure in future.

In this paper an empirical procedure of hull form improvement is developed, which is based on experimental results of series ship models and takes the resistance component due to FSSWs into account. Without comprehensive considerations of the resistance component due to FSSWs no satisfactory method of hull form improvement can be achieved, because every ship generates FSSWs, intensely or slightly depending on hull form and speed of advance.

* Graduate School, The University of Tokyo (present affiliation is Mitsui Engineering and Shipbuilding Co., Ltd.)

** Department of Naval Architecture, The University of Tokyo

This paper is composed mainly of two chapters. In Chapter 3 a method of extracting wave profiles of FSSWs from measured wave records is presented and a new parameter that denotes the magnitude of FSSWs is introduced with some applications to series models. A new design method for the sectional-area curve of minimum wave resistance is described in Chapter 4 together with the results of its application to a container hull form improvement.

2. Nomenclature

A_0 initial height of modeled FSSW profile
A' obtained height of modeled FSSW profile
a parameter of modeled FSSW profile
a_{0i}, a_{1i}, a_{2i} coefficients of quadratic approximation
B beam of ship
$C(\theta), S(\theta)$ amplitude functions
$C^*(\theta), S^*(\theta)$ weighted amplitude functions
$C_0^*(\theta), S_0^*(\theta)$ measured weighted amplitude functions of parent model
$C_j^*(\theta), S_j^*(\theta)$ do of j-th modified model on C_p-curve series
$\Delta C_j^*(\theta), \Delta S_j^*(\theta)$: $C_j^*(\theta)-C_0^*(\theta)$, $S_j^*(\theta)-S_0^*(\theta)$, respectively
$C_p(x)$ optimum sectional-area coefficient

$C_{p0}(x)$ sectional-area coefficient of parent model
$C_{pj}(x)$ do of j-th modified model
$\varDelta C_{pj}(x)$ $C_{pj}(x)-C_{p0}(x)$
C_w wave resistance coefficient obtained from towing test
C_{wp} wave-pattern resistance coefficient obtained from wave analysis
C_{ws} FSSW resistance coefficient given by C_w-C_{wp}
$\varDelta C_{wp}$ increment of wave-pattern resistance
$\varDelta C_w$ do of wave resistance
d draft
$E(x)$ error due to asymptotic expression at $y=0$
F_n Froude number based on L
$h(x)$ $\zeta_1^*-\zeta_0^*$
$\varDelta h$ magnitude of FSSW obtained from measured wave records
k_0 principal wave number
L ship length (between perpendiculars)
l $1/2\,L$
M number of tested ship models
N number of modified models
$P(\theta)$, $Q(\theta)$ amplitude functions
r correlation coefficient
U velocity of uniform flow
x, x' axis parallel to centerline of ship, aftward positive
y axis parallel to ship's beam, positive to starboard side
z vertical axis, upward positive
y_0 y-coordinate of base-line for longitudinal-cut
y_1 do of test-line
α_j coefficients
β shock angle of FSSWs
η_i y-coordinate of hull on load-water-line at i-th s.s., nondimensionalized by a half of beam length
η_{i0} η_i of parent model
η_{ij} η_i of j-th model
$\varDelta\eta_i$ $\eta_{ij}-\eta_{i0}$
ζ wave elevation
ζ_0 calculated wave height on the test-line derived from measured amplitude functions obtained on the base-line

(length including wave height is nondimensionalized by l unless otherwise defined.)

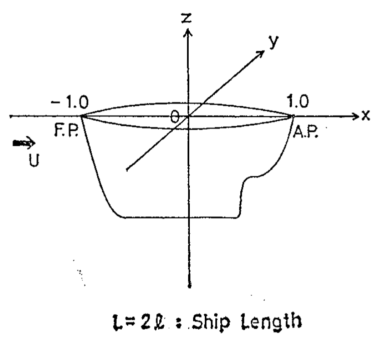

Fig. 1 Coordinate system

3. Extraction of FSSW profiles from measured wave records

It is important to clarify the relations between hull form and resistance due to FSSW experimentally at the first step of hull form improvement. Parameters indicating the magnitude of FSSWs must be introduced for quantitative treatments. The shock angle β, which varies with speed of advance, draft and entrance angle[4)5)6)], has been proposed as one of those parameters. However, shock angle alone does not always represent the magnitude of FSSWs satisfactorily in case the differences of hull form are relatively small. Another parameter which analogically corresponds to the jump of free surface across a shock front of shallow water shock wave comes to be important as a new parameter by which the magnitude of FSSWs can be expressed more precisely than shock angle.

3.1 Procedure of extraction

The procedure of extracting wave height due to FSSWs is shown in Fig. 2. There exist free wave, local-disturbance and FSSWs in the vicinity of a ship whereas at far away from the ship only free-wave exists. In order to exclude the local-disturbance, the method of longitudinal-cut wave analysis such as Newman-Sharma's method (abbreviated as N-S method) is available.

The procedure for extracting wave height due to FSSWs is as follows:

1) Choose two lines parallel to the centerline of ship as shown in Fig. 2. One is at a small distance from the centerline of the ship ($y=y_1$) where the magnitudes are to be evaluated (called test-line hereafter), and the other is at a sufficient distance from the ship ($y=y_0$) where the amplitude functions of free-wave are solely obtained (called base-line).

2) Calculate wave profiles on $y=y_1$ from the amplitude functions obtained on the two-different y-line, which are denoted by ζ_0^* and ζ_1^* as in Fig. 2. ζ_1^* contains free-wave and FSSWs while ζ_0^* contains only free-wave.

3) If $h(x)$ is defined by $\zeta_1^*-\zeta_0^*$, then $h(x)$ gives the approximate profile of FSSWs.

On calculating wave heights from amplitude functions, equivalent singularity distributions are not introduced, but the asymptotic expression at $y\to\infty$, that is,

$$\zeta=\int_0^{\pi/2}[C(\theta)\cos\{k_0\sec^2\theta(x\cos\theta+y\sin\theta)\\+S(\theta)\sin\{k_0\sec^2\theta(x\cos\theta+y\sin\theta\}]d\theta \quad (1.1)$$

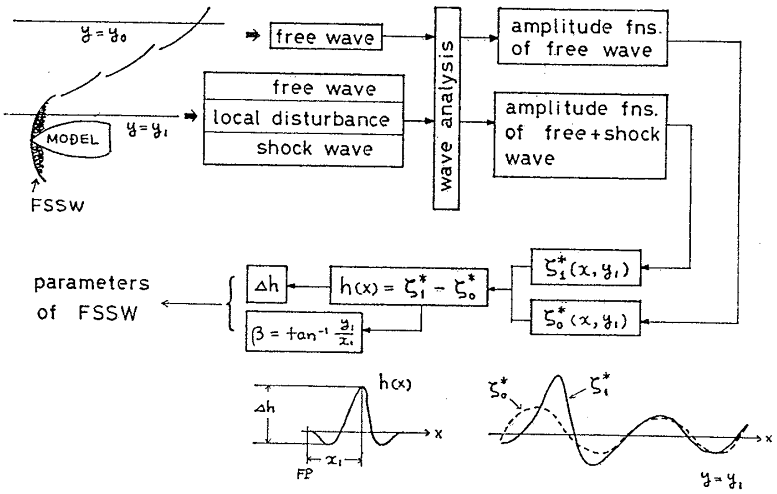

Fig. 2 Procedure of extracting wave profile of FSSW

is used, though it generates some errors in $h(x)$ because actually y is not large enough. The property of the error term is examined in the following section.

4) $h(x)$ is also directly obtained from difference of amplitude functions of the two different y-lines, y_0 and y_1, from Eq. (1.1). These differences of the amplitude functions are regarded as the amplitude functions due to FSSWs. They mostly appear in the high- θ region both in the case of modeled FSSWs and of actual ones.

5) Let Δh be the magnitude of pulse-like shape of $h(x)$ and be introduced as a new parameter in addition to the shock angle β.

3.2 Error due to asymptotic expression

The approximate method of extraction above-described is based on the following bold assumptions.

1) The interactions of free-waves with FSSWs are ignored,

2) Free-waves propagate linearly from the test-line ($y=y_1$) to the base-line ($y=y_0$).

The error which may arise through the process of calculating wave profiles on the test-line by amplitude functions at the base-line is considered small for our practical purposes, which is empirically studied in the following section.

In this section effects of some other errors are examined. Let the Cartesian coordinate system be fixed in a ship as shown in Fig. 1. At a great distance sideward from the ship, that is $y\to\infty$, the wave elevation can be expressed asymptotically as,

$$\zeta=\frac{k_0l}{\pi}\int_0^{\pi/2}[P(\theta)\cos\{k_0l\sec^2\theta(x\cos\theta+y\sin\theta)$$
$$+Q(\theta)\sin\{k_0l\sec^2\theta(x\cos\theta$$
$$+y\sin\theta)]\sec^3\theta d\theta \qquad (1.2)$$

Through Fourier transformation of ζ in Eq. (1.2) with respect to x, the relation between ζ and amplitude functions can be rewritten as follows:

$$P(\theta)+iQ(\theta)=\cos\theta\sin\theta\, e^{ik_0ly\tan\theta\sec\theta}$$
$$\times\int_{-\infty}^{\infty}\zeta(x,y)\,e^{ik_0lx\sec\theta}dx \qquad (1.3)$$

Let us examine the behavior of the error which may arise when Eq. (1.2) which is valid at infinity, is made use of at a certain finite y-coordinate. For simplicity assume that $y=0$ where the maximum error is to arise. Let ζ^* be a calculated wave profile on $y=0$ by substituting Eq. (1.3) into Eq. (1.2), ζ^* can be written as follows by changing variables in the way as $\omega=k_0l\sec\theta$,

$$\zeta^*=\frac{1}{\pi}\left[\int_{k_0l}^{\infty}d\omega\cos(\omega x)\int_{-\infty}^{\infty}\zeta(x',y)\cos(\omega x')dx'\right.$$
$$\left.+\int_{k_0l}^{\infty}d\omega\sin(\omega x)\int_{-\infty}^{\infty}\zeta(x',y)\sin(\omega x')dx'\right]$$
$$=\frac{1}{\pi}\left[\int_0^{\infty}d\omega\int_{-\infty}^{\infty}\zeta(x',y)\cos\{\omega(x-x')\}dx'\right.$$
$$\left.-\int_0^{k_0l}d\omega\int_{-\infty}^{\infty}\zeta(x',y)\cos\{\omega(x-x')\}dx'\right]$$
$$=\zeta-\frac{1}{\pi}\int_0^{k_0l}d\omega\int_{-\infty}^{\infty}\zeta(x',y)\cos\{\omega(x-x')\}dx' \qquad (1.4)$$

where Fourier double integral is considered. The 2nd term of R.H.S. of Eq. (1.4) is the error term caused by applying Eq. (1.2) on $y=0$.

It is clear from Eq. (1.4) that

$$\zeta^*\to\zeta \quad \text{if } k_0l\to0(F_n\to\infty)$$
$$\zeta^*\to0 \quad \text{if } k_0l\to\infty(F_n\to0)$$

Thus the error vanishes at the high speed limit whereas at the low speed limit, it has the same distribution as ζ with the opposite sign.

Provided ζ is the local-disturbance, it is desirable that $\zeta^*=0$ because it must be excluded for the present purpose. On the other hand, it is desired that $\zeta^*=\zeta$ when ζ is fully due to FSSWs. Therefore, there must be a certain limited region of Froude number for satisfactory extraction of FSSWs with a negligible influence of local disturbance[7)8)]. Some numerical experiments clarified that the influence of local disturbance on N-S method is sufficiently small in the range from $k_0L=10$ to 20, particularly in the high-θ region of amplitude functions where those due to FSSWs are mainly distributed.

Now, suppose that ζ represents a profile of FSSWs and assume the following simplified model of FSSW profile in order to examine the effects of longitudinal distribution of FSSW profile and of Froude number on the error term.

$$\zeta=A_0e^{-a^2(x-x_0)^2} \tag{1.5}$$

At $x=x_0$ the error term, $E(x_0)$, can be written as follows:

$$E(x_0)=-\frac{A_0k_0l}{\sqrt{\pi}\,a}\left\{1-\frac{1}{3\cdot2\cdot1}\left(\frac{k_0l}{2a}\right)^2+\frac{4}{5\cdot2^2\cdot2}\left(\frac{k_0l}{2a}\right)^4-\frac{8}{7\cdot2^3\cdot3!}\left(\frac{k_0l}{2a}\right)^6+\cdots\right\} \tag{1.6}$$

If the longitudinal distribution of a FSSW profile is narrower than about $1/5L_{pp}$ and $k_0L=10\sim20$, the error can be expressed approximately as

$$\frac{|E(x_0)|}{A_0}\propto\frac{k_0l}{a} \tag{1.7}$$

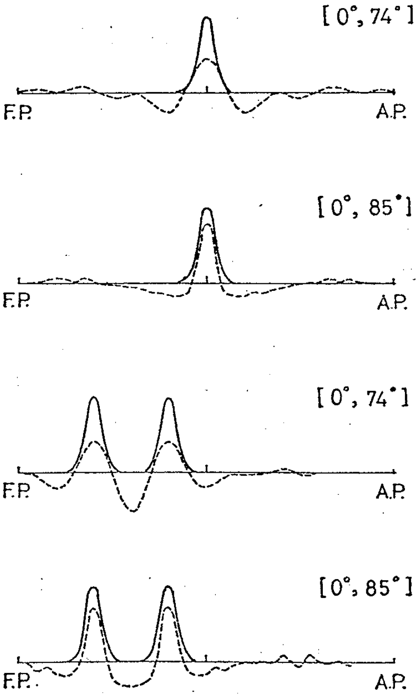

Fig. 3 Reproduction of a modeled FSSW

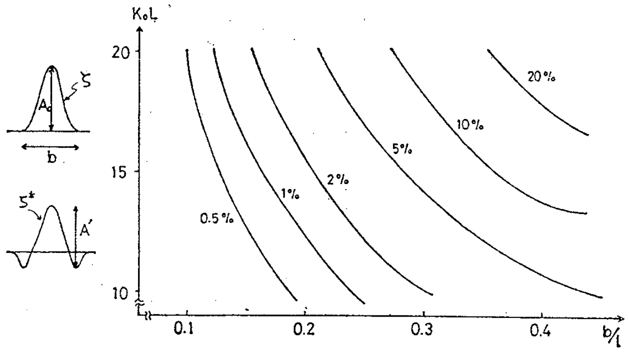

Fig. 4 $1-A'/A_0$

which shows that large F_n and/or narrow distribution of a FSSW profile give small value of error. The error term produces 'hollow parts' just beside the peak of FSSW profile as shown in Fig. 3. Let A' be the height of reproduced FSSW profile whose real height is A_0, the error in the height which is expressed by $1-A'/A_0$, is given as in Fig. 4. Comparisons of the height of FSSWs in the low speed range should be avoided because of the rapid growth of error according to the decrease of F_n. In the following analyses of measured wave records, A' is written as Δh and regarded as the height of FSSW on a y-line of interest.

3.3 Applications

(1) WM2

WM2 is a wall-sided model with parabolic waterlines given by

$$y=\frac{B}{2}(1-x^2), \quad B=1/5L \tag{1.8}$$

The maximum radius of bilge circle is 5 cm at midship. It is observed from wave pattern pictures shown in Fig. 5 that the pattern of FSSWs varies considerably with the change of draft.

Comparisons of $\zeta_1{}^*$ and $\zeta_0{}^*$ in case of $d=20$ cm at $F_n=0.26$ are shown in Fig. 6. Though three different base-lines are chosen in this case, they give similar $\zeta_0{}^*$, which means that waves propagate linearly on those lines and that any of the three lines is suitable for the base-line. On the other hand, a great difference between $\zeta_1{}^*$ and $\zeta_0{}^*$ is observed in the limited region near FP. It is considered to be caused by the existence of FSSWs and $h(x)=\zeta^*{}_1-\zeta_0{}^*$ gives a profile of FSSW at $y=y_1$ with 'hollows' which may be attributed to the error term.

The change of wave profile of FSSWs with the change of draft is well expressed by $\zeta_0{}^*$ and $\zeta_1{}^*$ as shown in Fig. 7. The backward shift of the longitudinal position of Wave-A according to the decrease of draft implies the decrease of the shock angle of Wave-A. The changes of $h(x)$

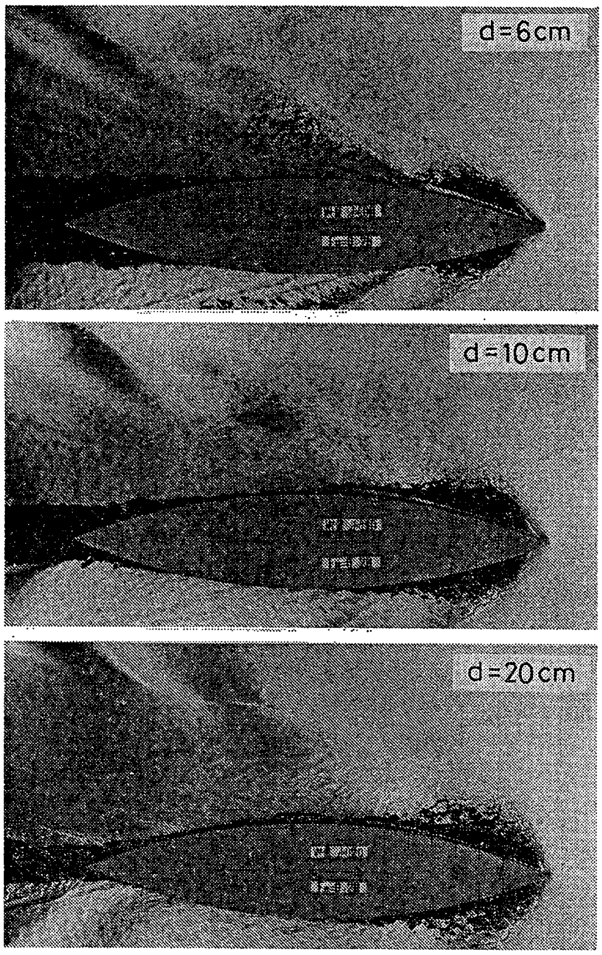

Fig. 5 Wave pattern pictures of WM2 at $F_n=0.26$

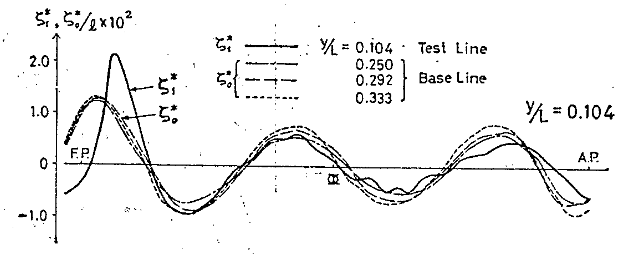

Fig. 6 ζ_1* and ζ_0* of WM2 at $F_n=0.26$, $d=20$ cm

due to the change of y-coordinate of the test-line are shown in Fig. 8 exemplifing the case of $d=$ 6 cm at $F_n=0.26$, in which one can see gradual diminishing of FSSWs with the increase of distance from the model.

(2) M46 sectional-area curve series

M46 sectional-area curve (C_p curve) series is composed of four ship models, i.e., the parent ship model M46, two other models M47 and M48 with modified C_p curves and M49 which was designed at $F_n=0.27$ to have minimum wave-pattern resistance by the method of Akashi Ship Model Basin[9] (abbreviated as ASMB). C_p curves of the fore-body are compared in Figs. 9 and 10. Aft-bodies are common to all models. They are semisymmetric models of a container hull form without bow bulb. The frame-lines are kept unvaried.

Entrance angles of M46~M49 are 11.4°, 8.1°, 13.1° and 11.0° respectively, if they are defined as $\tan^{-1} y/(^1/_{20} L_{pp})$, where y is the offset on load water line at s.s. $9^1/_2$. The obtained profiles of $h(x)$ of these models at $Fn=0.27$ are shown in Fig. 11. M48 with the largest entrance angle among the four generates Wave-A and Wave-B conspicuously, whereas they are so weak on M47 that Wave-B is almost indistinguishable. Although M49 has the C_p curve of minimum wave-

Table 1 Principal particulars

Model	M46	M47	M48	M49	M50	WM2		
Lpp (m)	2.0					2.4		
B (m)	0.3077					0.48		
d (m)	0.1047					0.20	0.10	0.06
L/B	6.5					5.0		
Cm	0.984					0.996	0.993	0.988
Cb	0.542					0.665	0.663	0.660
Cp	0.551					0.668		
∇ (m³)	0.03482	0.03482	0.03483	0.3484	0.3483	0.1532	0.0764	0.0456
S (m²)	0.6951	0.6961	0.6959	0.6963	0.6963	1.6645	1.1759	0.9839

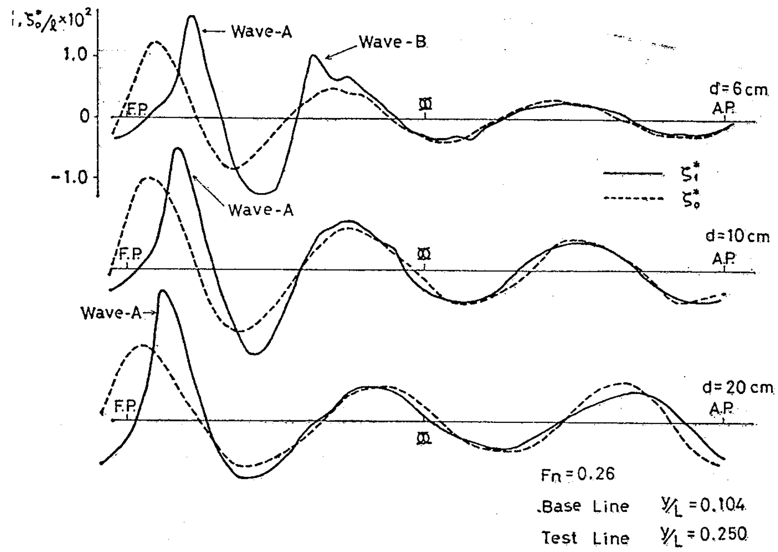

Fig. 7 ζ_1^* and ζ_0^* of WM2 at $F_n=0.26$

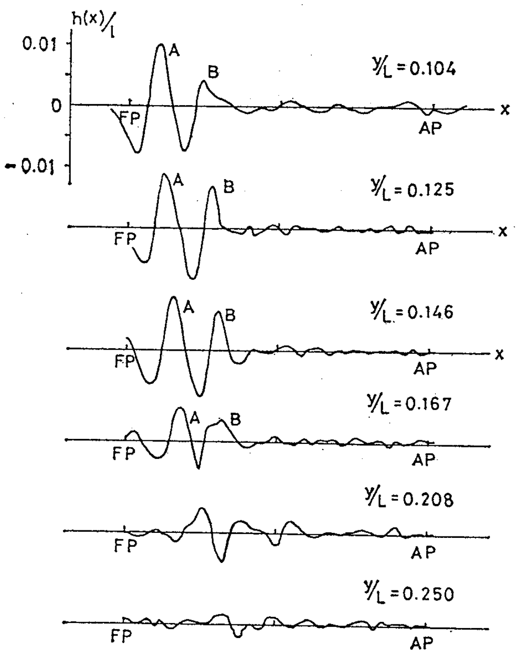

Fig. 8 $h(x)$ of WM2 at $F_n=0.22$, $d=6$ cm

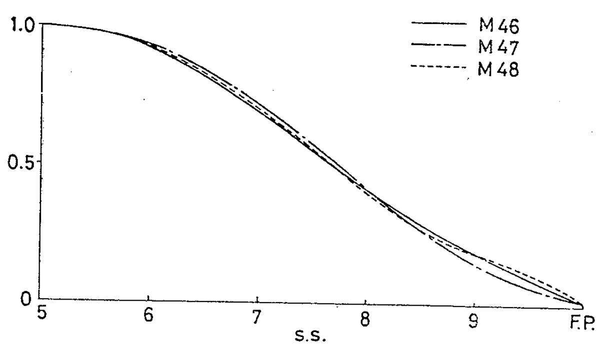

Fig. 9 Sectional area curves of M46, M47 and M48

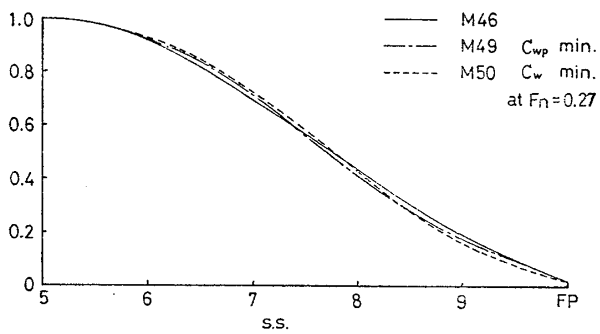

Fig. 10 Sectional area curves of M46, M49 and M50

pattern resistance, FSSWs are not reduced compared with those of the parent model M46, which suggests that the design method for the reduction of wave-pattern resistance is not sufficient for the reduction of wave-making resistance that includes FSSW resistance.

It is quite important that the profile of the FSSWs of M49 is similar to that of M46, since hull forms near the bow (FP∼s.s.9) are almost the same. Thus the local hull form near the bow gives dicisive effect on the generation of FSSWs.

3.4 Relation between Δh and C_w–C_{wp}

The new parameter Δh has intimate relation with the resistance due to FSSWs because it is an approximate strength of discontinuity. On the other hand, the resistance due to FSSW can be approximately derived by substracting C_{wp} from C_w, if superposition of resistance components is admitted. The relation between Δh of the foremost FSSW and C_w–C_{wp} is shown in Fig. 12, in which the correlation is simple and linear for series models with comparatively

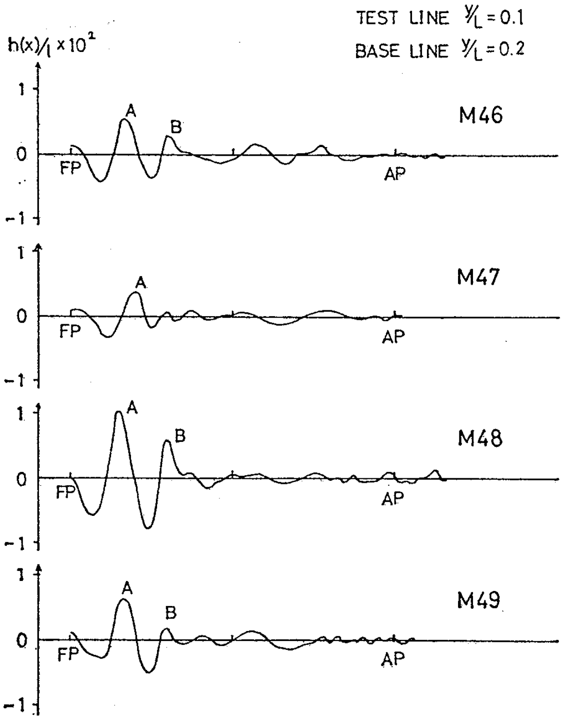

Fig. 11 $h(x)$ of M46~M49 at $Fn=0.27$

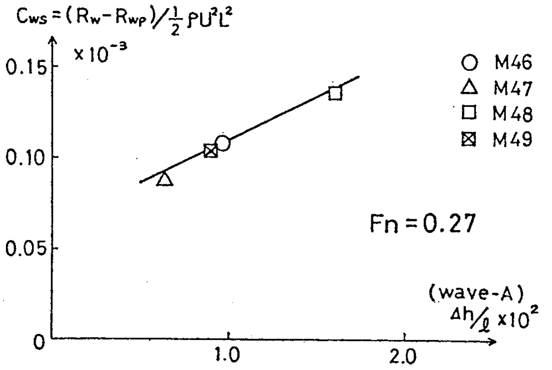

Fig. 12 Relation between Δh and C_w–C_{wp}

small modifications. This is very advantageous for C_w–C_{wp} to be considered as wave resistance due to FSSWs. In the following chapter this value is considered to express FSSW resistance for practical purposes. However, it should be noted that C_{wp} suffers scale effect, and consequently C_w–C_{wp}. This unfavorable effect would better be avoided by making use of larger model ships.

4. Method of optimizing C_p curves

4.1 Applications of the ASMB method[12]

The ASMB method[9] recently developed is based on wave analysis and aims at giving the optimum C_p curve of minimum wave-pattern resistance at a given F_n. Being different from other similar methods[10),11)], its theoretical construction seems to be simple without any ambiguous correction functions which will require a considerable amount of accumulated experimental data. This method is applied to the optimization of the C_p-curve of the fore-body of a container hull form and M49 is obtained at $F_n=0.27$ as shown in Fig. 10.

C_w from towing test (Schoenherr friction lines are used) and C_{wp} from N-S method of M46~M49 are shown in Fig. 13. M49 shows remarkable reduction in C_{wp} around design F_n. The measured weighted amplitude functions of M49 coincide well with the prediction, which ensures the propriety of the fundamental assumptions of the ASMB method. Nevertheless, C_w of M49 at $F_n=0.27$ remains almost the same with M47 whose C_{wp} is more than the double of M49. The reason is now clearly attributed to the resistance component due to FSSWs. M49 could not surpass M47 in C_w which has very weak FSSWs. Thus, in the second step, attempts should be

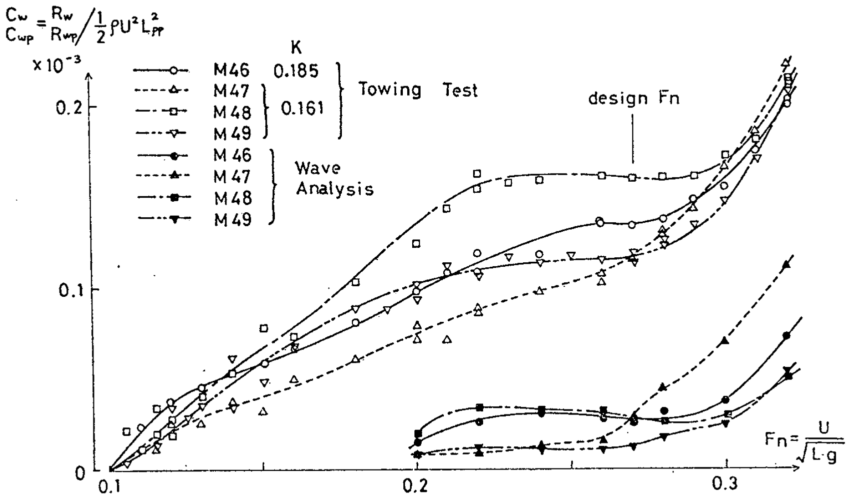

Fig. 13 C_w and C_{wp} curves of M46~M49 made for the finding of the optimum C_p curve of minimum C_w instead of C_{wp}.

4.2 Correlations between hull form and FSSW resistance

The effect of bulbs is not studied in this report but only that of C_p curves are discussed. C_p curves of M46 series straightly reflect on L.W.L. curves because of the invariability of their frame-lines. Let η_{ij} be offset on L.W.L. at i-th s.s. of j-th model and examine the relations between η_i near FP and FSSW resistance C_{ws} in terms of correlation coefficients assuming that C_{ws} is given by $C_w - C_{wp}$. Correlation coefficient of C_{ws} and η_i is defined as,

$$\gamma = D_1 / \sqrt{D_2 \cdot D_3} \tag{4.1}$$

where

$$\left.\begin{aligned} D_1 &= \sum_{j=1}^{M} (C_{ws,j} - \bar{C}_{ws})(\eta_{ij} - \bar{\eta}_i) \\ D_2 &= \sum_{j=1}^{M} (C_{ws,j} - \bar{C}_{ws})^2 \\ D_3 &= \sum_{j=1}^{M} (\eta_{ij} - \bar{\eta}_i)^2 \\ \bar{C}_{ws} &= \frac{1}{M} \sum_{j=1}^{M} C_{ws,j} \quad \bar{\eta}_i = \frac{1}{M} \sum_{j=1}^{M} \eta_{ij} \end{aligned}\right\} \tag{4.2}$$

As shown in Fig. 14-(a), γ is very close to 1 at any F_n within the region from s.s. 9 to FP. In other words, fine entrance reduces C_{ws} at any speed of advance, which is quite reasonable from the general properties of 'shock waves'.

On the other hand, correlations between C_{wp} and η_i, which are obtained from Eq. (4.1) by replacing C_{ws} by C_{wp}, vary considerably depending on F_n as shown in Fig. 14(b). In low and medium speed range, i.e, $F_n = 0.20 \sim 0.26$, hull forms having fine-entrance and hard-shoulder give smaller C_{wp}, while at $F_n = 0.27$ and 0.28, better results are expected by a little fuller entrance, and at $F_n = 0.30$ the hull form of full-entrance and easy-shoulder is desired for smaller C_{wp}. (It is noted that full-entrance gives easy-shoulder and vise versa since the displacement is assumed constant.) Such tendency is well known in terms of linear wave resistance theory. It should be noted that two relations, C_{ws} vs. η_i and C_{wp} vs. η_i, have the same tendency of reducing resistance when F_n is smaller than 0.26 but that they conflict each other in the higher speed range where the optimization should be carried out so as to minimize the sum of both components i.e. C_w.

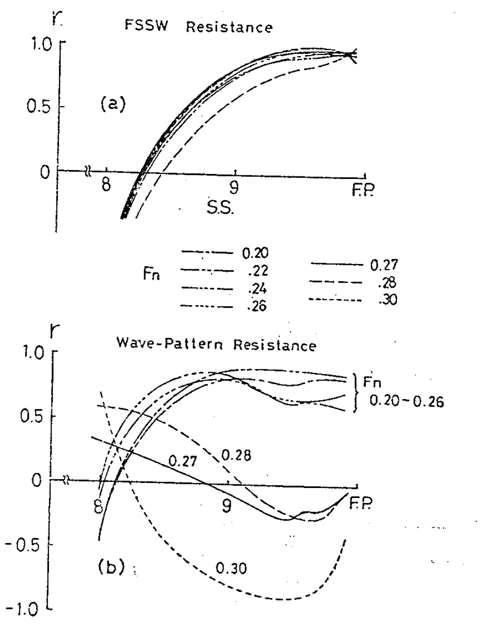

Fig. 14 Correlation coefficients

The informations obtained here explain the quantitative difference of C_w curves and C_{wp} curves which can be seen in Fig. 13. It is frequently observed in tank test results of C_p curve series models that the model with a fine entrance keeps superiority in C_w in the wider range of advance speed, whereas its superiority in C_{wp} ceases at a comparatively low advance speed. In Fig. 13, M47 shows smallest C_w in the range $F_n < 0.27$, while it is overcome in C_{wp} in the range $F_n > 0.23$ by M49. Since fine-entrance reduces FSSW resistance at any F_n, it plays a role of suppressing the rise of C_w curves and consequently brings forth the above tendency.

4.3 Method of minimizing the sum of linear and nonlinear wave resistance

For the sum of wave pattern resistance (linear wave resistance) and resistance due to FSSW (nonlinear wave resistance) to be minimized, the correlation between hull form and resistance component due to FSSW (C_{ws}) is incorporated into the ASMB method as follows.

1) Obtain the relations between C_{ws} and η_i at several s.s. near F.P. from experimental results on C_p curve series and approximate the relations in the following quadratic form.

$$C_{ws} = a_{0i} + a_{1i}\eta_i + a_{2i}\eta_i^2 \tag{4.3}$$

Coefficients a_{0i}, a_{1i} and a_{2i} are determined by the method of least square. For M46 series, quadratic approximations are given at four s.s. as shown in Fig. 15 in which M43E3 has similar particulars to those of M46 series but with the entrance angle of 15°.

2) Express the optimum C_p curve at a certain F_n as,

$$C_p(x) = C_{p0}(x) + \sum_{j=1}^{N} \alpha_j \Delta C_{pj}(x) \tag{4.4}$$

Since frame-lines are not modified, η_i is given as

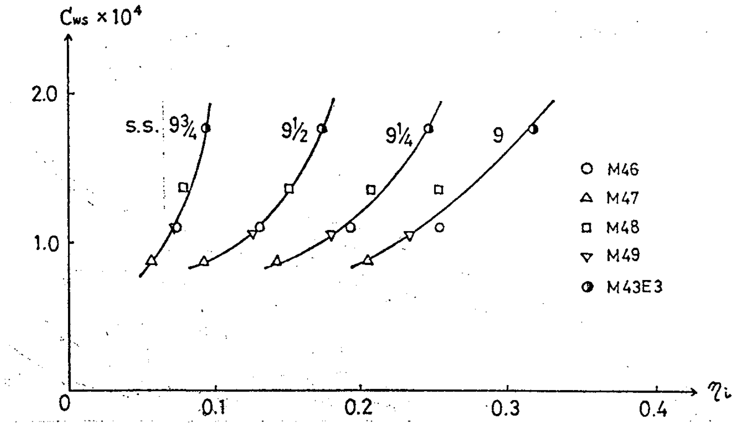

Fig. 15 C_{ws} vs. η_i

$$\eta_i=\eta_{i0}+\sum_{j=1}^{N}\alpha_j\Delta\eta_{ij} \qquad (4.5)$$

Then the increment of C_w is expressed as

$$\Delta C_w=4\pi\int_0^{\pi/2}\left[\sum_{j=1}^{N}\alpha_j\left(\frac{C_0^*}{L}\cdot\frac{\Delta C_j^*}{L}+\frac{S_0^*}{L}\cdot\frac{\Delta S_j^*}{L}\right)\right]d\theta+2\pi\int_0^{\pi/2}\left[\left(\sum_{j=1}^{N}\alpha_j\frac{\Delta C_j^*}{L}\right)^2+\left(\sum_{j=1}^{N}\alpha_j\frac{\Delta S_j^*}{L}\right)^2\right]d\theta+a_{1i}\sum_{j=1}^{N}\alpha_j\Delta\eta_{ij}+a_{2i}(\eta_{i0}+\sum_{j=1}^{N}\alpha_j\Delta\eta_{ij})^2-2a_{2i}\eta_0^2 \qquad (4.6)$$

The first and second terms are for ΔC_{wp} in the ASMB method. α_j of minimum C_w is determined by,

$$\frac{\partial\Delta C_w}{\partial\alpha_j}=0 \qquad j=1, N \qquad (4.7)$$

which leads to the following simultaneous equations.

$$\begin{Bmatrix}\alpha_1\\ \alpha_2\\ \vdots\\ \alpha_N\end{Bmatrix}=\begin{bmatrix}A_{11} & A_{12}\cdots\cdots A_{1N}\\ A_{21} & A_{22}\cdots\cdots A_{2N}\\ \vdots & \vdots \quad \ddots \quad \vdots\\ A_{N1} & A_{N2}\cdots\cdots A_{NN}\end{bmatrix}^{-1}\begin{Bmatrix}B_1\\ B_2\\ \vdots\\ B_N\end{Bmatrix} \qquad (4.8)$$

where

$$A_{kj}=4\pi\int_0^{\pi/2}\left(\frac{\Delta C_k^*}{L}\cdot\frac{\Delta C_j^*}{L}+\frac{\Delta S_k^*}{L}\cdot\frac{\Delta S_j^*}{L}\right)d\theta+2a_{2i}\Delta\eta_{ik}\eta_{ij} \qquad (4.9a)$$

$$B_k=-4\pi\int_0^{\pi/2}\left(\frac{C_0^*}{L}\cdot\frac{\Delta C_k^*}{L}+\frac{S_0^*}{L}\cdot\frac{\Delta S_k^*}{L}\right)d\theta-2a_{1i}\Delta\eta_{ik}-2a_{2i}\eta_{i0} \qquad (4.9b)$$

3) When the relation between C_{ws} and η_i (Eq. (4.3)) is obtained at four square stations, for instance, four sets of $\{\alpha_j\}$ and sixteen estimated values of C_{ws} are obtained. Thus sixteen values of C_w are estimated which is the sum of C_{ws} and C_{wp}, though C_{wp} has four different estimations. Among several sets of $\{\alpha_j\}$, one should choose one set which gives as a whole small values of C_w. Actually, however, little difference is found among the obtained optimum C_p curves. It is helpful for this choice to make use of the correlation ratio around quadratic of Eq. (4.3).

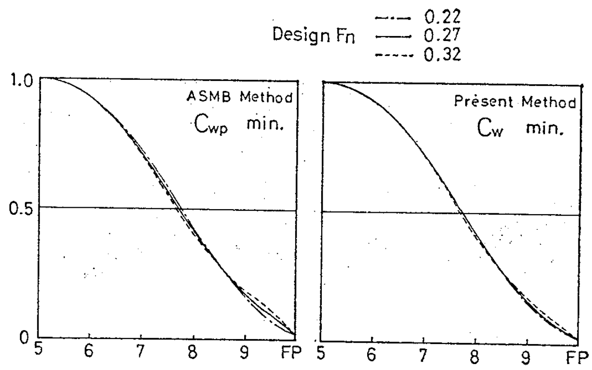

Fig. 16 Optimum sectional area curves

4.4 Optimum C_p Curves

Optimization schemes for C_p curves were carried out by both the ASMB method and the present one at several design Froude numbers from 0.20 to 0.32. Three of these are exemplified in Fig. 16. The optimum C_p curve of minimum C_w is less influenced by the change of design speed and keeps a tendency of fine-entrance with hard-shoulder up to the high-speed region because of the consideration of FSSW resistance. These results are expected from the correlations shown in Fig. 14 as well.

Based on the optimum C_p curve of minimum C_w at $F_n=0.27$, M50 was prepared to ascertain the availability of the present method.

4.5 Tank test results of M50

C_w and C_{wp} curves of M50 are shown in Fig. 17 together with those of M49. M50 achieves a

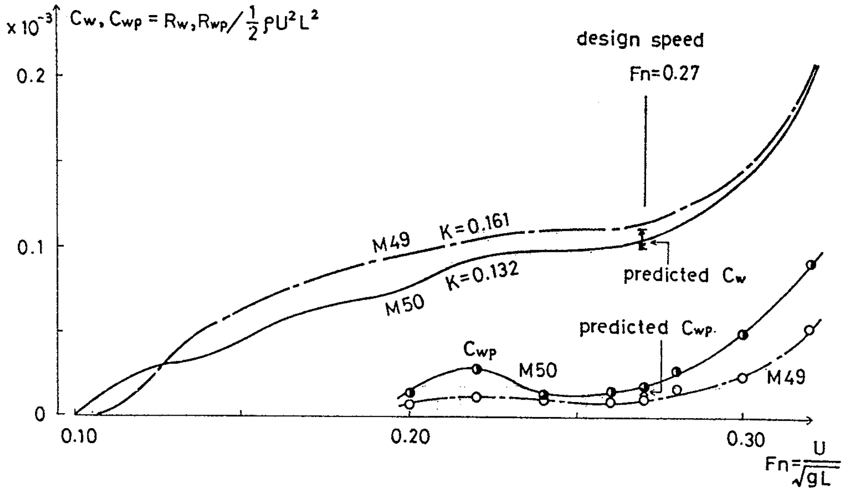

Fig. 17 C_w and C_{wp} curves of M47～M50

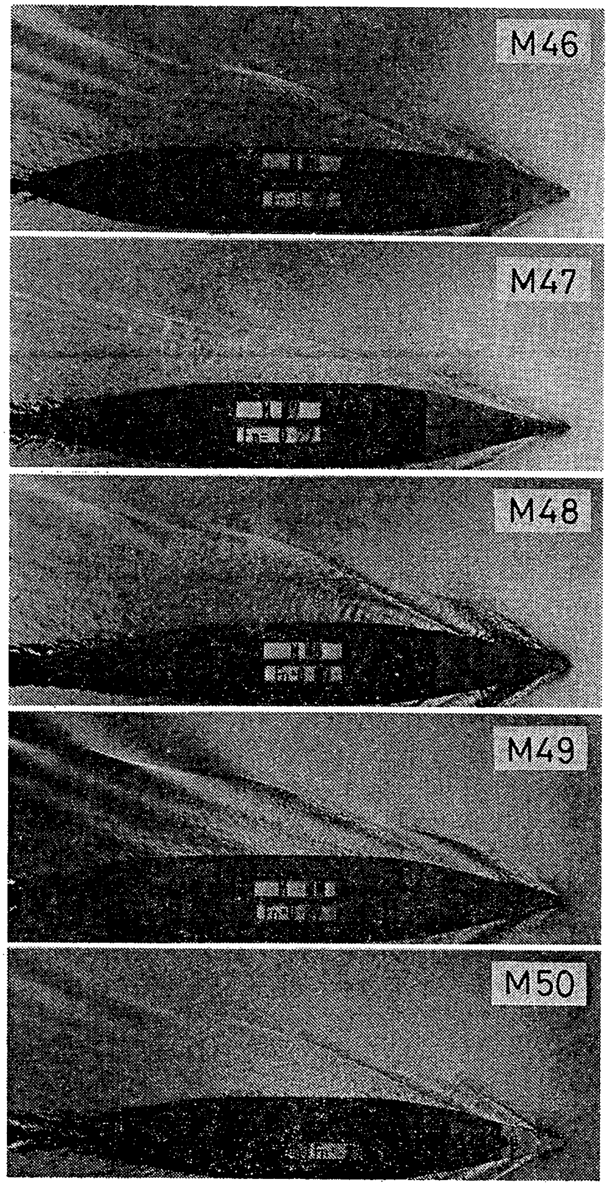

Fig. 18 Wave pattern pictures of M46 series at $F_n=0.27$

9.4% reduction of C_w compared to M49 at $F_n=0.27$, which is just within the prediction of from 2.6% to 12.8%. Relatively small C_{wp} is simultaneously obtained at $F_n=0.27$ which is predicted with a considerable degree of accuracy. These facts indicate the effectiveness of the present method to reduce C_w, as well as the effectiveness of the ASMB method to reduce C_{wp}.

Wave-pattern pictures of M46 series are shown in Fig. 18. The magnitude of FSSWs of M50 should be smaller than M49 and larger than M47, which is observed well in these pictures.

5. Conclusion

Principal conclusions are as follows:

1) A method for the extraction of FSSW profiles from measured wave records is developed, wherein a new parameter Δh that indicates the magnitude of FSSW is introduced.
2) Local hull form near the bow has dominant influences on FSSWs.
3) A new design method for hull forms of minimum wave resistance is developed by incorporating the correlation between hull form and resistance due to FSSW into the ASMB method. The effectiveness of this method is demonstrated by the application to hull form of a container carrier.
4) In general, the superiority of fine-entrance with hard-shoulder holds up to the high-speed region when the resistance component due to FSSW is taken into consideration.

This research is partly supported by the Grant-in-Aid for Scientific Research of the Ministry of Education, Science and Culture.

References

1) Inui, T., Kajitani, H., Miyata, H. et al.: Nonlinear Properties of Wave Making Resistance of Wide-Beam Ships, J. of Soc. of Naval Arch. of Japan, Vol. 146 (1979).
2) Miyata, H., Inui, T., Kajitani, H.: Free Surface Shock Waves around Ships and Their Effects on Ship Resistance, J. of Soc. of Naval Arch. of Japan, Vol. 147 (1980)
3) Kawamura, N., Kajitani, H., Miyata, H.: Experimental Investigation on the Resistance Component due to Free Surface Shock Waves on Series Ship Models, J. of Kansai Soc. of Naval Arch., Japan, Vol. 179 (1980).
4) Miyata, H., Suzuki, A., Kajitani, H.: Numerical Explanation of Nonlinear Nondispersive Waves around Bow, Proc. of Third International Conference on Numerical Ship Hydrodynamics (1981).
5) Miyata, H.: Characteristics of Nonlinear Waves in the Near-Field of Ships and Their Effects on Resistance, Proc. of 13th Symposium on Naval Hydrodynamics, Tokyo, Japan (1980).
6) Takahashi, M., Kajitani, H., Miyata, H.: Characteristics of Free Surface Shock Waves around Wedge Models, J. of Soc. of Naval Arch. of Japan, Vol. 148 (1980).
7) Maruo, H., Ikehata, M.: Determination of Wave-Making Resistance of a Ship by the Method of Wave Analysis (3rd Report), J. of Soc. of Naval Arch. of Japan, Vol. 126 (1969).
8) Eggers, K., Kajitani, H.,: A Component Concerning Local-Wave Influence on Longitudinal-Cut Wave Analysis, presented to 12th ITTC, Rome (1969).
9) Matsui, M., Tsuda, T., Ohkubo, K., Asano, S.: A Method for Optimization of Ship Hull Forms based on Wave-Pattern Analysis Data, J. of Soc. of Naval Arch. of Japan, Vol. 147 (1980).
10) Baba, E.: An Application of Wave Pattern Analysis to Ship Form Improvement, J. of Soc. of Naval Arch. of Japan, Vol. 132 (1972).
11) Tsutsumi, T.: An Application of Wave Resistance Theory to Hull Form Design, J of Soc. of Naval Arch. of Japan, Vol. 144 (1978).
12) Masuko, A., Yamamoto, H.: An Application of Wave Analysis to Hull Form Design, graduation thesis of the University of Tokyo, (1980).

7), 9) and 12) are written in Japanese.